

Temperature dependent selective crystallization behavior of iPP with  $\beta$   
nucleating agent

Ziwei Cai<sup>1</sup>, Yao Zhang<sup>1</sup>, Jingqing Li<sup>1</sup>, Yingrui Shang<sup>1</sup>, Hong Huo<sup>2</sup>, Jiachun Feng<sup>3</sup>,  
Sergio S. Funari<sup>4</sup>, Shichun Jiang<sup>\*1</sup>

<sup>1</sup> School of Materials Science and Engineering, Tianjin University, Tianjin 300072, P.  
R. China

<sup>2</sup> Institute of Polymer Chemistry and Physics, College of Chemistry, Beijing Normal  
University, Beijing 100875, PR China

<sup>3</sup> Key Laboratory of Molecular Engineering of Polymers of Ministry of Education,  
Department of Macromolecular Science and Laboratory of Advanced Materials,  
Fudan University, Shanghai 200433, P. R. China

<sup>4</sup> HASYLAB at DESY, Notkestraße 85, D-22607 Hamburg, Germany

---

\* Corresponding author: [scjiang@tju.edu.cn](mailto:scjiang@tju.edu.cn)

## Abstract

Crystallization behavior of isotactic polypropylene (iPP) induced with aryl amide derivative (TMB-5) as  $\beta$ -form nucleating agent at different temperatures were investigated via synchrotron small angle and wide angle X-ray scattering (SAXS/WAXS) and polarized optical microscopy (POM). The WAXS results indicated that TMB-5 is a temperature dependent selective nucleating agent for iPP crystallization. In another words, only  $\beta$ -crystal or  $\alpha$ -crystal forms at low or high crystallization temperature, both  $\beta$ -crystal and  $\alpha$ -crystal can be found at proper crystallization temperature. A possible mechanism was proposed to understand the phenomenon and crystallization behavior of iPP with nucleating agent.

**Keywords:** iPP; selective nucleating agent; crystallization

## Introduction

The applicable properties of crystalline polymers are determined by their final formed structures and the process of structure formation. The processing and structure of crystalline polymers are attracting interests from researchers due to its promising performances. Isotactic polypropylene(iPP) is a commonly used semicrystalline polymer, which can form several crystal modifications: monoclinic ( $\alpha$ ), trigonal ( $\beta$ ), orthorhombic ( $\gamma$ ) form, and smectic mesophase[1-3]. The monoclinic  $\alpha$  phase is the dominating crystal modification when the polymer material solidifies from the melt under ordinary conditions. The  $\beta$  form is usually induced by flow or  $\beta$ -nucleating agents. The  $\gamma$  form is preferentially formed from crystallization under pressure [4]. Under certain conditions, e.g. undercooling, a mesophase usually referred to as ‘smectic’ is formed instead of crystalline phase [5].

In the past decades numerous research groups dedicated considerable efforts to the preparation of the  $\beta$ -modification of isotactic polypropylene ( $\beta$ -iPP), because of its excellent mechanical properties. Varga reported differences in physical properties between  $\alpha$  and  $\beta$  forms of iPP [6, 7]. It has been reported that comparing to the  $\beta$  form,  $\alpha$  form shows higher modulus and tensile strength, and inferior fracture toughness. The impact strength and toughness of  $\beta$ -iPP exceed those of  $\alpha$ -iPP. The improved mechanical performance of  $\beta$ -iPP makes it very attractive for numerous applications [8,9]. The production of  $\beta$ -iPP requires the presence of  $\beta$ -nucleating agents, which have high activity, selectivity, and sufficient physical and chemical stability. Amount

of the  $\beta$  crystal might be increased under some special conditions such as shearing [10-12] or elongation of the melt during crystallization, directional crystallization in a temperature gradient field, quenching the melt to a certain temperature range, vibration-induced crystallization, and addition nucleating agents into the sample [13]. Though implementation of efficient and selective  $\beta$ -nucleants is the most reliable method for preparation of samples rich in  $\beta$ -modification Varga has demonstrated that calcium pimelate and suberate are the highest selective among all known  $\beta$ -nucleating agents [14].

It is known that specific crystals can be induced by addition of specific nucleating agents ( $\alpha$ - or  $\beta$ - nucleating agent in the case of iPP) [15-19]. However, this method is too complex and difficult to manipulate for commercial products. The selective nucleating agent is attractive for obtaining ideal materials of iPP with designed proportional  $\alpha$  and  $\beta$  form crystals via simple and convenient approach. In this study, aryl amide derivative (TMB-5) was used as nuclei for iPP crystallization. TMB-5 was reported as a nonselective nucleating agent for iPP with melting point of 197°C. Both  $\alpha$  and  $\beta$ -iPP can be found in the presence of TMB-5. This behavior of TMB-5 was termed as dual nucleating ability [20]. It is an aromatic amide derivative with similar chemical structures to some aromatic amine  $\beta$ -nucleating agents. Although temperature related studies on the similar nucleating and iPP systems have been done by some other researchers and they did well [21-24], our results have great industrial interest. The detailed study related to the dual nucleation of TMB-5 indicated it is a temperature dependent selective nucleating agent for iPP crystallization. The WAXS results indicated that only  $\beta$ -crystal or  $\alpha$ -crystal forms at low or high crystallization temperature, both  $\beta$ -crystal and  $\alpha$ -crystal can be found at proper crystallization temperature. Taking advantage of this excellent feature, we can adjust the temperature to get a certain kind of iPP which we want.

## Experimental Section

### Materials

The iPP used in this study is a commercial product of Aldrich Chemical Company, Inc. The  $M_w$  and  $M_n$  are  $3.4 \times 10^5$  g/mol and  $7.4 \times 10^4$  g/mol, measured by gel permeation chromatography(GPC). The melting point of iPP is around 165°C. TMB-5 was supplied by Chemical Institute of Shanxi, China. According to the reference, the

chemical structure is shown in Figure 1 [23].

### **Sample preparation**

iPP granules and TMB-5 powder were put into the 60 mL chamber of an XSS-300 torque rheometer together and melt-mixed at 190 °C for 10 min with a rotation speed of 30 rpm. The obtained iPP/TMB-5 blends were soon sampled and then molded into 1 mm thick sheets. The concentrations of the nucleating agent were 0.05, 0.1, 0.2, 0.5, and 1 wt % and the samples were designated as PP1, PP2, PP3, PP4 and PP5, respectively. The pure iPP sample designated as PP0 was prepared in an identical process for comparison.

### **Synchrotron SAXS and WAXS measurements**

X-ray scattering experiments were performed using synchrotron radiation with  $\lambda = 0.150$  nm at Beamline A2 of HASYLAB (Hamburg, Germany) for simultaneous SAXS/WAXS measurements and synchrotron radiation with  $\lambda = 0.154$  nm at Beamline 4B9A of Beijing Synchrotron Radiation Facility (Beijing, China) for WAXS measurements with Mar165 CCD detector. Two linear position-sensitive detectors were used, one of them covering approximately the  $2\theta$  range from 10 to 30° and the other being set at a 230 cm sample-detector distance in the direction of the beam at A2. The aluminum foil packed samples for in situ synchrotron investigation were heated to 220°C kept at 220 °C for 5 min to eliminate the thermal history before it was cooled down to isothermal crystallization temperatures as soon as possible with the temperature controller at Beamline A2 and the cooling rate was 30 °C/min with Linkam heat stage at Beamline 4B9A. The synchrotron SAXS/WAXS data were recorded as soon as the temperatures cool down to the isothermal crystallization temperatures.

### **Polarizing microscope (POM)**

An Olympus POM (TH4-200) equipped with a Q-imaging color video camera and Linkam optical high-temperature stage (TST 350, England) was used to observe the crystallization morphology in isothermal crystallization progress of iPP/TMB-5 blends. The samples for POM observation were heated to 220°C on the hot stage at the ramping rate of 30 °C/min. The sample was kept at 220 °C for 5 min to eliminate the thermal history before it was cooled down to 25°C, 135°C, 140°C, 145°C and 150°C at the rate of 30 °C/min.

### **Evaluation of the $\beta$ -modification**

The relative amount of  $\beta$ -modification can be estimated from the K-values of the

samples. The relative amount of the  $\beta$ -phase K-values in the crystalline portion of the material has been evaluated by the method of Turner-Jones et al. [25]

$$K=I(300)_\beta/(I(300)_\beta+I(110)_\alpha+I(040)_\alpha+I(130)_\alpha) \quad (1)$$

where  $I(110)$ ,  $I(040)$ , and  $I(130)$  are the intensities of the three strongest equatorial peaks of  $\alpha$ -form attributed to the (110), (040) and (130) planes of monoclinic cell, respectively. While  $I(300)$  is the intensity of the strongest diffraction peak of the trigonal  $\beta$ -form. The K value is zero in the absence of the  $\beta$ -form and unity if only the  $\beta$ -form is present.

## Results and Discussion

To measure the  $\beta$ -phase content in crystallized iPP samples, WAXS ( $\lambda= 0.150$  nm) profiles are analyzed and the relative fractions of  $\beta$ -iPP are obtained. Fig. 2 shows the WAXS ( $\lambda= 0.150$  nm) profiles of iPP/TMB-5 blends with various TMB-5 concentrations crystallized at room temperature. It is observed that the WAXS profile of pure iPP shows four obvious peaks at  $2\theta$  values  $13.9^\circ$ ,  $16.5^\circ$ ,  $18.2^\circ$ , and  $21.3^\circ$ , which correspond to the (110), (040), (130), and (131) diffraction, respectively. These characteristic diffraction peaks indicate that only  $\alpha$ -monoclinic crystal form exists in the pure iPP sample. In the figure we can see that even at a low concentration of TMB-5 (0.05 wt%), there is an obvious peak at about  $16^\circ$  which corresponds to the (300) diffraction of  $\beta$ -trigonal crystal form, indicating  $\beta$ -crystal form exists in the samples. From Fig. 2, we can see that the diffraction intensity of the  $\beta$  marker peak increased with the nucleating agent. It implies the increase of the portion of  $\beta$ -phase and the decrease of  $\alpha$ -phase amount in the specimen. This result also shows that TMB-5 can induce iPP to form  $\beta$  crystals effectively.

Understanding in the nucleation from  $\beta$ -nucleating agent for iPP crystallization is important in both scientific research and commercial applications. However, the mechanism of nucleating agent induced crystallization of  $\beta$ -iPP is still not well understood. The '*dimensional lattice matching theory*' proposed by Lotz et al.[26,27] has been widely accepted for some  $\beta$ -nucleating agents of iPP. In this theory, it explained the  $\beta$ -iPP nucleating ability by analyzing the structure relationship between nucleating agent and the  $\beta$ -form iPP. A lattice matching between c-axis periodicity of iPP ( $6.5 \text{ \AA}$ ) and a corresponding distance in the substrate crystal face of nucleating agent is the main reason for inducing the  $\beta$ -form iPP polymorph. The nucleating

agents provide the nucleation surfaces for iPP crystal. Kawai et al.[28] proposed the equation of misfit factor ( $f_m$ ) between the two crystal structures of iPP and the nucleating agent which can be calculated as

$$f_m = (PB-PA)/PA*100\% \quad (2)$$

where PA and PB are the appropriate period length of substrate and polymer, respectively. If  $f_m < 15\%$ , the epitaxy is considered to be good. The  $f_m$  between the layer spacing of TMB-5 and the c-axis of iPP is 2.9%, indicating excellent epitaxy. According to Kawai et. al. [28], the c-axis of the iPP aligns parallel to the b-axis of the TMB-5. It was concluded that the bc-plane of the TMB-5 crystal is the epitaxial surface onto which the (330)  $\beta$  plane of the  $\beta$ -phase iPP grows. Analysis of the molecular packing of the iPP helix onto the epitaxial surface determined in his study revealed that the  $\beta$  phase exhibits a good fit to this surface, while  $\alpha$  phase does not.

Analysis of the relationship between the polymeric nucleating agents and  $\beta$ -crystal structure helps determining the structural requirements for nucleating agent. The  $\beta$ -modification of iPP has a trigonal unit cell with parameters  $a = b = 1.101$  nm and  $c = 0.65$  nm, which contains three isochiral helices. This cell is frustrated: the three helices do not have similar azimuthal orientations [29]. It does not comply with the rules of classical crystallography, which postulates structural equivalency. Different nucleating agents can induce these helical chains organizing into several different spatial arrangements and giving rise to distinct polymorphs [30]. According to Su et. al. [30], the polymers with  $\beta$ -nucleating activity all have benzene rings in their molecular structure. The benzene rings of the polymeric nucleating agents may act as a growth surface of crystal and induce the helix chains of iPP epitaxial crystallize on it. Moreover, some polar functional groups (such as  $-\text{CONH}-$ ) may enhance the  $\beta$ -nucleating activity of iPP [30]. As shown in Fig. 1, the chemical structure of TMB-5 constitutes of both  $-\text{CONH}-$  and benzene rings. Therefore TMB-5 is very effective on inducing higher level of  $\beta$ -crystal form in iPP under the crystallization condition.

It is known that thermal history has influence on the crystallization behavior and structure of crystalline polymers [31-36]. The changes in crystal forms between  $\alpha$  and  $\beta$  for iPP have been studied by many researchers and the difference of crystallization between the  $\alpha$  and  $\beta$  forms are strongly related to the kinetics of the crystallization. For example,  $\alpha$  form crystals with  $\beta$  nucleating agents generate at higher crystallization temperature,  $\beta$  form is crystallized at lower temperature, and  $\alpha$  forms generate again at the crystallization temperature below about 80°C. These changes in

the crystal forms could be related to the difference of the crystal growth rates of  $\alpha$  and  $\beta$  forms at each crystallization temperature. Therefore, we track TMB-5 induced isothermal crystallization process of iPP with synchrotron SAXS/WAXS measurements. The WAXS ( $\lambda=0.150$  nm) profile of iPP/ TMB-5 blends with different TMB-5 content isothermally crystallized at 135°C and 140°C were obtained and the final results of the samples are shown in Fig. 3. From the results in Fig. 3a, we can see that when the concentration of TMB-5 is below 0.2wt%, only the typical peaks of  $\beta$ -crystal at about 15.8° are observable. The peak at  $2\theta$  of approximately 14.0°, which corresponds to the (110) diffraction for  $\alpha$ -crystal, can be seen when nucleating agent constant is higher than 0.2%. However, the intensity of this peak is very faint. From the results in Fig. 3b, one can see that the intensity of the  $\beta$  form crystal diffraction increased with the concentration of the nucleating agent, which indicates the  $\beta$  crystal increase with the nucleating agent. In this figure we can also see that at a low concentration of nucleating agent (0.05 wt%), there are visible peaks at about 14.0°, 16.5° and 18.2°, which correspond to the (110), (040) and (130) diffraction of  $\alpha$  crystal form, indicating the exist of  $\alpha$ -crystal form in the sample. In iPP6 (iPP/TMB-5 (1wt %)),  $\beta$ -nucleating agent provides a large amount of heterogeneous nucleation sites for the growth of  $\beta$ -crystals, so the typical diffraction characteristic of the  $\beta$ -iPP modification is clearly observed. Meanwhile relatively low intensity diffraction peaks that correspond to the  $\alpha$  crystal of iPP can be observed at the same profile.

The crystallization of both  $\alpha$  and  $\beta$  form at 140°C with TMB-5 were investigated with WAXS. The crystalline morphology images with various nucleating agent obtained from POM are shown in Fig. 4. It can be observed that the spherulite size of pure iPP (PP0) is larger than that in iPP samples with TMB-5.

The spherulite growth in pure iPP is mainly a nucleation-controlled homogeneous nucleation of crystallization. Therefore, the spherulite of iPP can grow very large before it impinges on another spherulite. While in iPP with nucleating agent, a large number of nuclei would be induced by nucleating agent. The spherulite cannot grow large enough to overlap, increased nucleus density results in a significant decrease in the average size of the spherulites.

The nucleation and growth mechanism are sensitive to the concentration of TMB-5, discuss in the earlier section, and causes the relative change (the increase of the numbers and the decrease of the size of spherulites) in crystalline modification (Fig. 4) to vary with the conditions adopted for the investigation. This is confirmed by the

result of WAXS.

To determine the evolution of  $\beta$ -crystals with fixed crystallization temperature, the intensity of  $\beta$  marker peak from WAXS ( $\lambda = 0.150$  nm) and SAXS ( $\lambda = 0.154$  nm) as a function of crystallization time are present in Fig. 5. One can find from Fig. 5 that the crystallization rate increase with the concentration of TMB-5. It can be seen that for different TMB-5 concentrations, the intensity of  $\beta$  peaks increases with time. It turns out that the addition of TMB-5 agent facilitated the formation of  $\beta$  phase. On the other hand, the intensity becomes stable beyond a certain time. Meanwhile the maximum intensity of the peaks for  $\beta$  phase are identical for all samples, implies that the increase of TMB-5 composition in iPP will not affect the ratio of the  $\beta$  phase in the stable state of the crystallization.

Both  $\alpha$  and  $\beta$  crystals are based on the same three-fold helical conformation of the chain. The heat distortion temperature of  $\beta$ -phase exceeds that of  $\alpha$ -iPP [7]. Therefore,  $\beta$ -iPP is the metastable phase (it melts at  $< 155^\circ\text{C}$  as opposed to  $< 170^\circ\text{C}$  for  $\alpha$ -iPP), and growth rate is higher (by up to 70%) than that of  $\alpha$ -iPP over most of the ‘usual’ crystallization temperature range (i.e., between 100 and 140  $^\circ\text{C}$ ). Within this limited range of crystallization temperature, a high content of  $\beta$ -iPP can be obtained. Therefore, for the present samples of iPP, blending with an appreciable amount of TMB-5, the formation of the  $\beta$  crystal form is thermodynamically favored in the temperature range from 100 to 140 $^\circ\text{C}$ . Moreover, the most favorable temperature for  $\beta$ -form growth is near 135 $^\circ\text{C}$ . So when iPP/TMB-5 crystallized at 135 $^\circ\text{C}$ , the content of  $\beta$  crystal form is high and little  $\alpha$ -crystal form can be found in the sample. Crystallization is an exothermic process, thus the value of enthalpy ( $\Delta H$ ) is negative. In comparison with  $\alpha$ -iPP, formation of  $\beta$ -iPP has higher enthalpy ( $\Delta H_\alpha = 170$  J/g;  $\Delta H_\beta = 168.5$  J/g) [7]. Thermodynamically the phase which has a lower enthalpy ( $\Delta H$ ) is more favorable. Moreover, as reported by Varga [37], and on account of its higher melting temperature,  $\alpha$ -iPP grows faster than  $\beta$ -iPP at high temperatures, above a critical temperature  $T_c$  (140 $^\circ\text{C}$ ). Therefore at higher crystallization temperatures the crystallization of metastable  $\beta$ -crystal form is slow because of its lower supercooling temperature ( $T_m - T_c$ ) and fusion enthalpy, while the  $\alpha$ -form becomes more stable and kinetically favorable. Therefore, the  $\alpha$ -crystal form increases with crystallization temperature in iPP/TMB-5 systems. From the above discussion, it is reasonable to conclude that the crystalline temperature is a crucial element on the final

crystallization structure of iPP for iPP/TMB-5 systems.

It is known that crystallization temperature has influence on the polymer crystallization behavior and structure of crystalline polymers. The nucleation and growth rate of the  $\beta$  phase in iPP/TMB-5 are very sensitive to the concentration of TMB-5. The content of the  $\beta$  phase increases with TMB-5 percentage as shown in Fig. 3. However, the peaks in WAXS profile resulted from  $\alpha$ -crystal of iPP can be found as shown in Fig. 3a even the crystallization temperature is 135°C with concentration of TMB-5 higher than 0.2wt%. Only  $\beta$ -crystal of iPP can be induced as shown in the WAXS profile (Fig. 3a) with concentration of TMB-5 lower than 0.2wt%. This phenomenon is not consistent with the reported results [21, 23], because TMB-5 was considered as a  $\beta$  nucleating agent. As shown in Fig. 4 and 5, the numbers of spherulites and the rate of crystallization increased with the concentration of TMB-5. Crystallization process is an exothermic process. The increase in the number of spherulites originated from the increase of TMB-5 induced nuclei and led to the increase in the crystallization rate and exothermic heat. The exothermic heat which cannot be spread out in time would lead to rise the local crystallization temperature. Kayo NAKAMURA et al [38] studied the crystal growth rate of  $\alpha$  and  $\beta$  forms in a wide range of crystallization temperatures. In his paper, they indicated that the ratio of crystals growth rates ( $G_{\beta}/G_{\alpha}$ ) varies with crystallization temperature. Intersection of crystal growth rate from  $\beta$  to  $\alpha$  form ( $G_{\alpha} > G_{\beta}$ ) has been observed at about 140°C. On the other hand, in the temperature range below about 105°C, it has been predicted that  $G_{\alpha}$  becomes faster again than  $G_{\beta}$ . And these crossover temperatures may be different with a difference in isotacticity. So the rise of the local crystallization temperature can promote the crystal growth rate of  $\alpha$  from which results in the formation of  $\alpha$ -crystal. In addition, crystal density would be increased with nuclei and then the interaction between spherulites increases in fixed volume. The densities of the  $\alpha$ -phase and  $\beta$ -phase are 0.949 g cm<sup>-3</sup> and 0.939 g cm<sup>-3</sup>, respectively, according to close match of the melting temperatures of the corresponding crystalline phases with those in the literature [13]. The increase of the crystal density is preferred to form  $\alpha$ -phase because of the greater density of  $\alpha$ -phase. Therefore, we are convinced of crystallization temperature is the dominating element for TMB-5 induced iPP crystallization with selectivity. This phenomenon is confirmed by the final WAXS profiles of iPP/TMB-5 blends isothermally crystallized at 135°C and 140°C (Fig. 3), especially the results in Fig. 7 (the samples crystallized at 145°C).

The relationship between the relative amount  $\beta$ -content and the nucleating agent can be determined by K-value according to WAXS results. Generally speaking, the increase of concentration of the nucleating agents helps to increase the proportion of  $\beta$ -crystals;  $\beta$ -nucleating agent provided a large amount of heterogeneous nucleation sites for the growth of  $\beta$ -crystals. The  $K_{\beta}(300)$  calculated by WAXS ( $\lambda= 0.150$  nm) data are plotted in Fig. 6 as a function of nucleating agent content. From the results in Fig. 6 one can find that the  $\beta$ -form of the samples containing  $\beta$ -nucleating agent increases rapidly until the agent content is more than 0.2% and then slightly increases with continuously increasing agent content. That shows a critical nucleation concentration. The dependence of the  $K_{\beta}(300)$  values on the concentration of nucleating agents had been investigated by several researchers and the similar trend was observed [30,39-41]. Su et al.[30] thought that it can be explained by the changes of dispersibility of polymeric nucleating agents in iPP matrix. The dispersibility of polymeric nucleating agents heavily depends on the concentration of nucleating agents and the mixing method.

To demonstrate the influence of temperature on the nucleation of TMB-5, we investigated the samples crystallized at higher temperatures via in situ synchrotron SAXS/WAXS measurements. Fig. 7 shows the WAXD ( $\lambda= 0.150$  nm) patterns of nucleated iPP with different TMB-5 contents crystallized at 145°C. From the results in Figure 7, we can see that when the samples crystallized at 145°C, only  $\alpha$ -monoclinic crystal form exists in the observed iPP sample, which is also different from that crystallized at 135°C and 140°C.

TMB-5 is an effective  $\beta$  form nucleating agent for iPP above a critical concentration, but it is not completely selective, certain amount of  $\alpha$ -phase can be detected in all samples. This behavior of TMB-5 is termed as dual nucleating ability. This is also confirmed by Varga in his previous paper [37]. He also proved that TMB-5 is not a selective  $\beta$ -nucleating agent due to the partial  $\alpha$ -nucleating effect of its lateral crystal surface. This  $\alpha$ -nucleating effect can be shown also directly in his PLM micrographs. Therefore, it is suitable to be used to investigate the crystallization and transition behaviors of iPP. However, according to our experimental results, we consider that TMB-5 is a temperature-dependent selective nucleating agent. Under different temperature conditions, TMB-5 plays different roles in promoting the nucleation. When iPP/TMB-5 blends crystallized at 135°C, TMB-5 only to promote the nucleation of the  $\beta$  phase; When crystallized at 140°C, TMB-5 stimulates the

nucleation of the  $\beta$  phase together with  $\alpha$  phase; When the temperature is above 140°C, TMB-5 only has a role in promoting the nucleation of the  $\alpha$  phase.

## Conclusions

In the current study, the nucleating ability of TMB-5 towards isotactic polypropylene (iPP) and its effects on the content of  $\beta$ -crystal, and crystallization behavior of iPP under isothermal crystallization process were investigated. The experimental results indicate TMB-5 is a temperature-dependent selective nucleating agent for iPP crystallization. In another words, only  $\beta$ -crystal or  $\alpha$ -crystal forms at the crystallization temperature of 135°C or 145°C, both  $\beta$ -crystal and  $\alpha$ -crystal can be found at 140°C. The changes in crystal forms are strongly related to the kinetics of the crystallization. That is, at different crystallization temperature with TMB-5 which is a temperature-dependent selective nucleating agent,  $\alpha$  and  $\beta$  forms have different crystal growth rates.

## Acknowledgement

This work was supported by National Natural Science Foundation of China (50773082, 20974077, 20804005, 50903061) and the Fundamental Research Funds for the Central Universities.

## References

1. Liu, M. X.; Guo, B. C.; Du, M. L.; Chen, F.; Jia, D. M. *Polymer* 2009, 50, 3022-3030.
2. Menyhardt, A.; Gahleitner, M.; Varga, J.; Bernreitner, K.; Jääskeläinen, P.; Øysæd, H.; Pukánszky, B. *Eur. Polym. J.* 2009, 45, 3138-3148.
3. Zhang, P. Y.; Liu, X. X.; Li, Y. Q. *Mater. Sci. Eng., A.* 2006, 434, 310-313.
4. Hoyos, M.; Tiemblo, P.; Gómez-Elvira, J. M. *Eur. Polym. J.* 2009, 45, 1322-1327.
5. Lezak, E.; Bartczak, Z.; Galeski, A. *Polymer* 2006, 47, 8562-8574.
6. Chen, H. B.; Karger-Kocsis, J.; Wu, J. S.; Varga, J. *Polymer* 2002, 43, 6505-6514.
7. Varga, J. *J. Macromol. Sci., Phys.* 2002, 41, 1121-1171.
8. Shangguan, Y. G.; Song, Y. H.; Peng, M.; Li, B. P.; Zheng, Q. *Eur. Polym. J.* 2005, 41, 1766-1771.

9. Han, L.; Li, X. X.; Li, Y. L.; Huang, T.; Wang, Y.; Wu, J.; Xiang, F. M. *Mater. Sci. Eng., A*. 2010, 527, 3176-3185.
10. Li, H. H.; Zhang, X. Q.; Duan, Y. X.; Wang, D. J.; Li, L.; Yan, S. K. *Polymer* 2004, 45, 8059-8065.
11. Li, H.; Zhang, X.; Kuang, X.; Wang, J.; Wang, D.; Li, L.; Yan, S. *Macromolecules* 2004, 37, 2847-2853.
12. Chen, Y. H.; Mao, Y. M.; Li, Z. M.; Hsiao, B. S. *Macromolecules* 2010, 43, 6760-6771.
13. Li, J. X.; Cheung, W. L. *Polymer* 1999, 40, 2085-2088.
14. Menyárd, A.; Varga, J.; Molnár, G. J. *Therm. Anal. Calorim.* 2006, 83, 625-630.
15. Romankiewicz, A.; Sterzynski, T.; Brostow, W. *Polym. Int.* 2004, 53, 2086-2091.
16. Nezbedova, E.; Pospisil, V.; Bohaty, P.; Vlach, B. *Macromol. Symp.* 2001, 170, 349-357.
17. Cho, K.; Saheb, D. N.; Choi, J.; Yang, H. *Polymer* 2002, 43, 1407-1416.
18. Yang, Z. G.; Mai, K. C. J. *Appl. Polym. Sci.* 2011, 119, 3566-3573.
19. Qin, J.; Chen, X. L.; Yu, J.; Wang, Y.; Tian, Y. Z.; Wu, S. J. *Appl. Polym. Sci.* 2010, 117, 1047-1054.
20. Varga, J.; Menyárd, A. *Macromolecules* 2007, 40, 2422-2431.
21. Dong, M.; Guo, Z. X.; Yu, J.; Su, Z. Q. *J. Polym. Sci., Part B: Polym. Phys.* 2008, 46, 1725-1733.
22. Dong, M.; Jia, M. Y.; Guo, Z. X.; Yu, J. *Chin. J. Polym. Sci.* 2011, 29, 308-317.
23. Dong, M.; Guo, Z. X.; Yu, J.; Su, Z. Q. *J. Polym. Sci., Part B: Polym. Phys.* 2009, 47, 314-325.
24. Dong, M.; Guo, Z. X.; Su, Z.; Yu, J. *J. Appl. Polym. Sci.* 2011, 119, 1374-1382.
25. Turner-Jones, A.; Aizlewood, J. M.; Beckett, D. R. *Macromol. Chem. Phys.* 1964, 75, 134-159.
26. Lotz, B. *Polymer* 1998, 39, 4561-4567.
27. Mathieu, C.; Thierry, A.; Wittmann, J. C.; Lotz, B. *Polymer* 2000, 41, 7241-7253.
28. Kawai, T.; Iijima, R.; Yamamoto, Y.; Kimura, T. *Polymer* 2002, 43, 7301-7306.
29. Xu, W.; Martin, D. C.; Arruda, E. M. *Polymer* 2005, 46, 455-470.
30. Su, Z. Q.; Dong, M.; Guo, Z. X.; Yu, J. *Macromolecules* 2007, 40, 4217-4224.
31. Yuan, Q.; Rajan, V. G.; Misra, R. D. K. *Mater. Sci. Eng., B*. 2008, 153, 88-95.
32. Medellin-Rodriguez, F. J.; Mata-Padilla, M.; Mata-Padilla, S.; Vega-Diaz, S.; Davalos-Montoya, O. J. *Polym. Sci., Part B: Polym. Phys.* 2008, 46, 2188-2200.

33. Menyhárd, A.; Varga, J.; Liber, Á.; Belina, G. *Eur. Polym. J.* 2005, 41, 669-677.
34. Li, X. X.; Wu, H. Y.; Wang, Y.; Bai, H. W.; Liu, L.; Huang, T. *Mater. Sci. Eng., A.* 2010, 527, 531-538.
35. Menyhárd, A.; Varga, J. *Eur. Polym. J.* 2006, 42, 3257-3268.
36. Yang, Z. G.; Zhang, Z. S.; Tao, Y. Z.; Mai, K. C. *J. Appl. Polym. Sci.* 2009, 112, 1-8.
37. Varga, J.; Mudra, I.; Ehrenstein, G. W. *J. Therm. Anal. Calorim.* 1999, 56, 1047-1057.
38. Kayo, N.; Satoko, S.; Susume, U.; Annette, T.; Bernard, L.; Norimasa, O. *Polymer J.* 2008, 40, 915-922.
39. Zhao, S. C.; Cai, Z.; Xin, Z. *Polymer* 2008, 49, 2745-2754.
40. Huo, H.; Jiang, S. C.; An, L. *J. Macromolecules* 2004, 37, 2478-2483.
41. Xiao, W. C.; Wu, P. Y.; Feng, J. C. *J. Appl. Polym. Sci.* 2008, 108, 3370-3379.

Captions:

Figure 1 Chemical structure of N,N'-dicyclohexyl-2,6-naphthalenedicarboxamide (DCNDCA).

Figure 2 WAXD patterns of sample PP0 (pure iPP) and nucleated iPP with different TMB-5 contents at room temperature under quiescent condition.

Figure 3 WAXD patterns of sample PP0 (pure iPP) and nucleated iPP with different TMB-5 contents crystallized at 135 °C (a) and 140 °C (b).

Figure 4 Micrographs for pure iPP and nucleated iPP sample crystallized at 135 °C: (a) pure iPP, (b) 0.05, (c) 0.1, (d) 0.2, (e) 0.5, (f) 1 wt%.

Figure 5 The time dependent scattering intensity of samples isothermally crystallized at 135 °C (a:  $2\theta=15.8$  obtained from WAXS ( $\lambda=0.150$  nm) profiles; b:  $s=0.046$  nm<sup>-1</sup> obtained from SAXS ( $\lambda=0.150$  nm) profiles).

Figure 6  $K_{\beta(300)}$  value and  $K_{\alpha(110)}$  value as a function of TMB-5 content.

Figure 7 WAXD patterns of nucleated iPP with different TMB-5 contents crystallized at 145 °C.

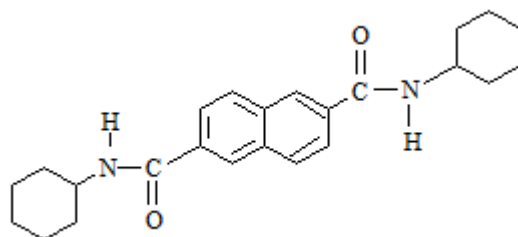


Figure 1 Chemical structure of N,N'-dicyclohexyl-2,6-naphthalenedicarboxamide (DCNDCA).

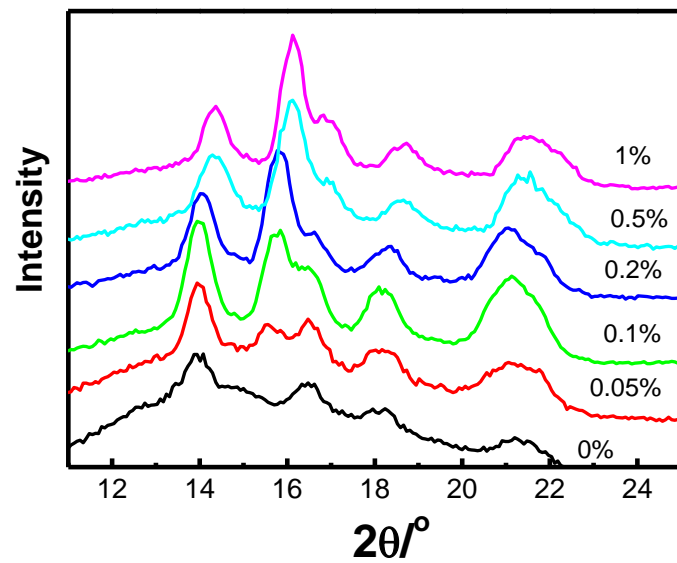


Figure 2 WAXD( $\lambda= 0.150$  nm) patterns of sample PP0 (pure iPP) and nucleated iPP with different TMB-5 contents at room temperature

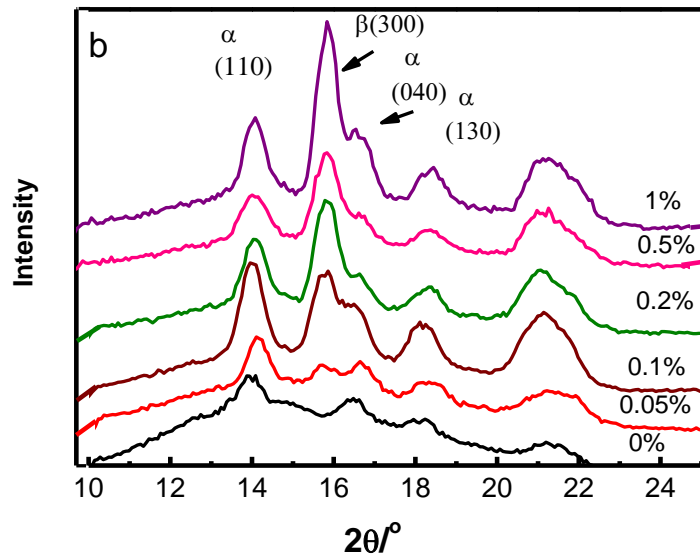
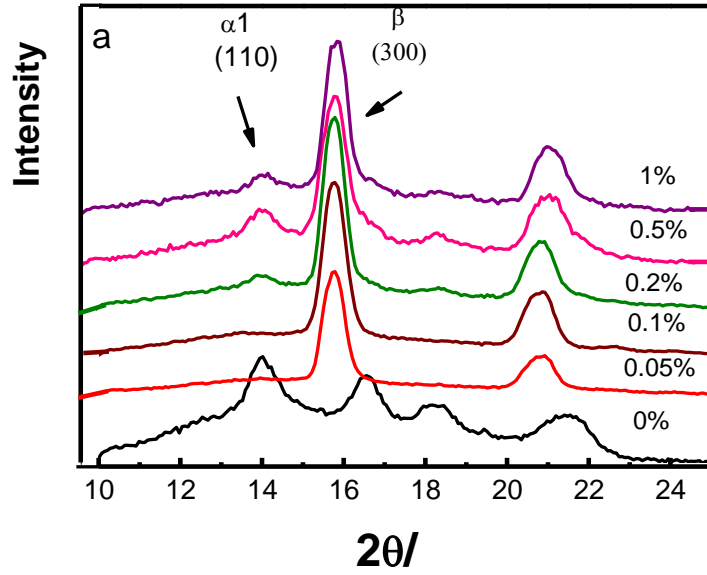


Figure 3 WAXD( $\lambda= 0.150$  nm) patterns of sample PP0 (pure iPP) and nucleated iPP with different TMB-5 contents crystallized at 135 °C (a) and 140 °C(b).

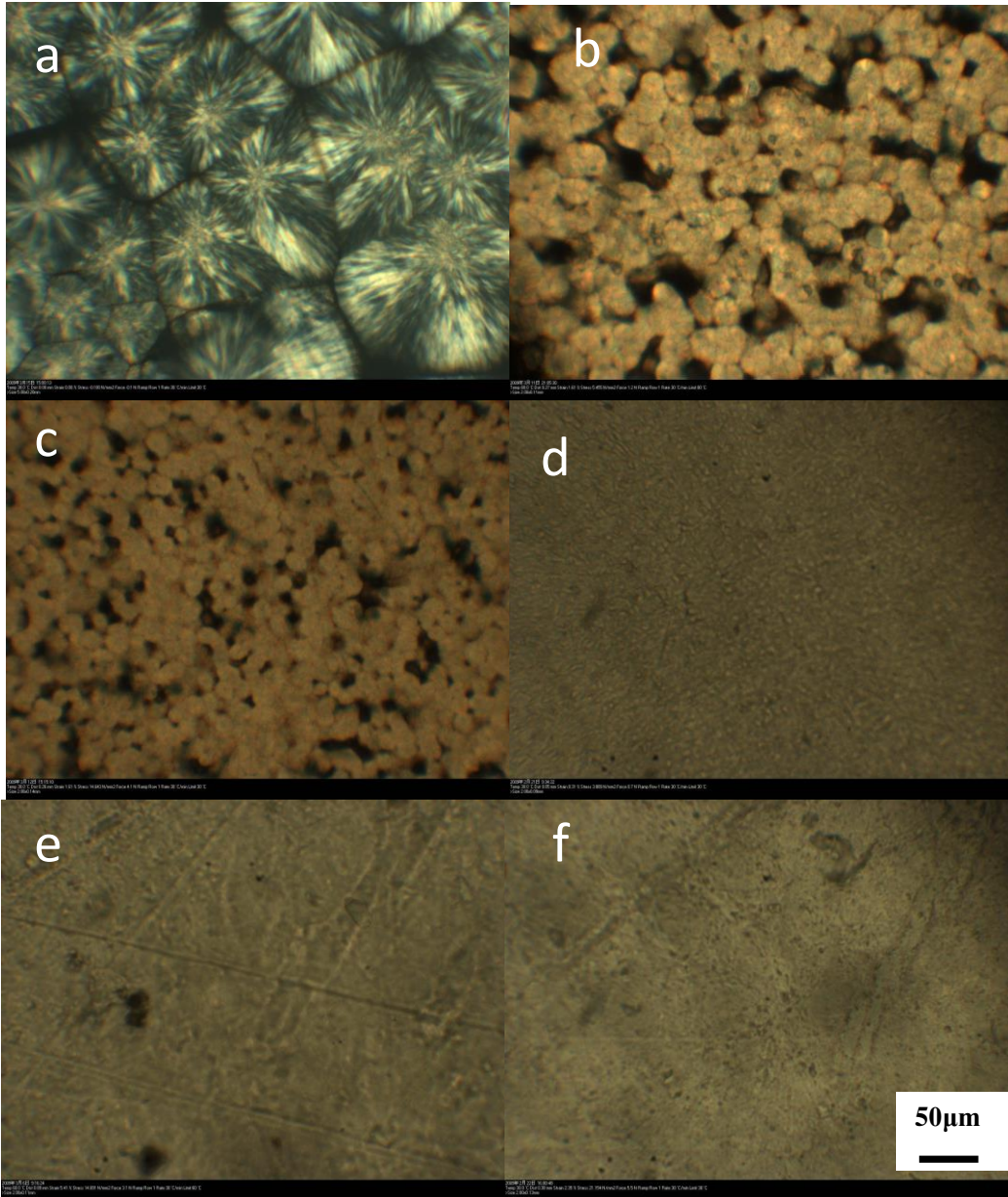


Figure 4 Micrographs for pure iPP and nucleated iPP sample crystallized at 135 °C: (a) pure iPP, (b) 0.05, (c) 0.1, (d) 0.2, (e) 0.5, (f) 1 wt%

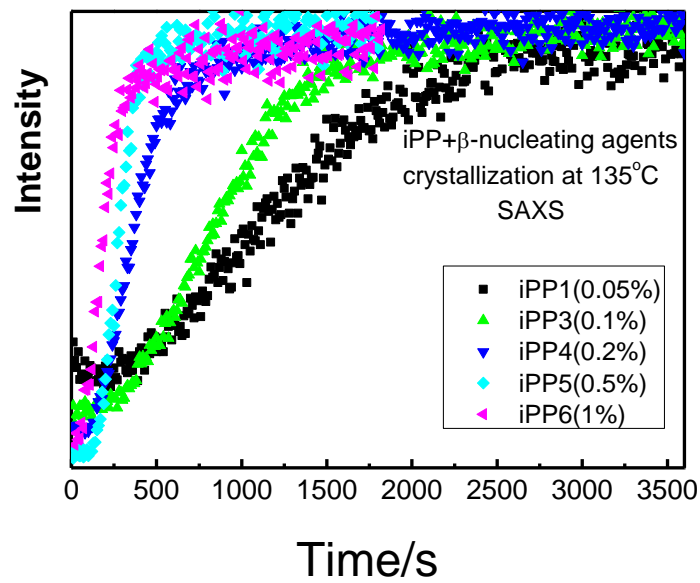
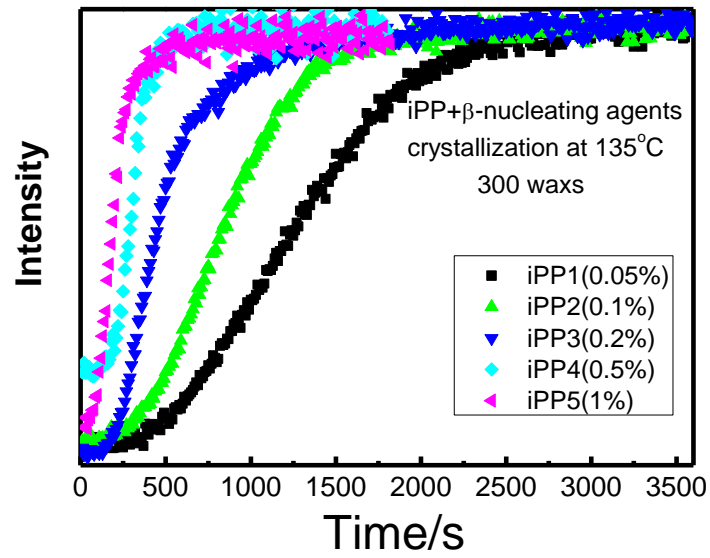


Figure 5 The time dependent scattering intensity of samples isothermally crystallized at 135°C (a:  $2\theta=15.8$  obtained from WAXS ( $\lambda= 0.150$  nm) profiles; b:  $s=0.046$  nm<sup>-1</sup> obtained from SAXS ( $\lambda= 0.150$  nm) profiles).

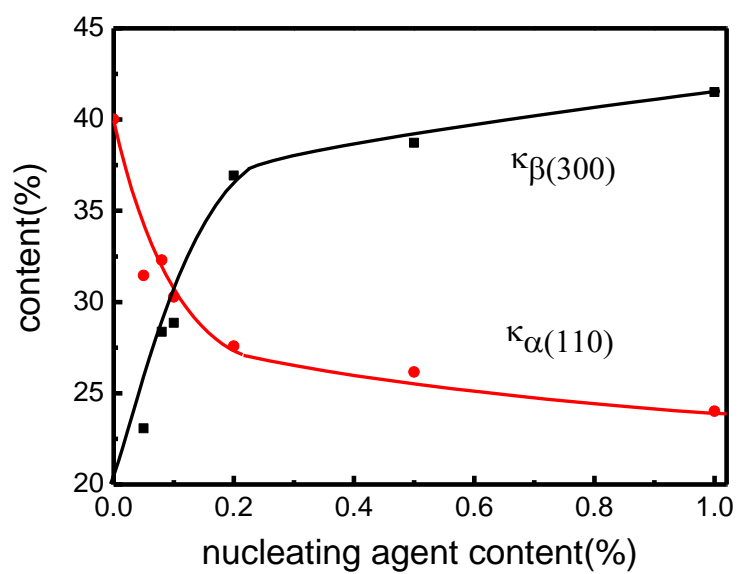


Figure 6  $K_{\beta(300)}$  value and  $K_{\alpha(110)}$  value as a function of TMB-5 content

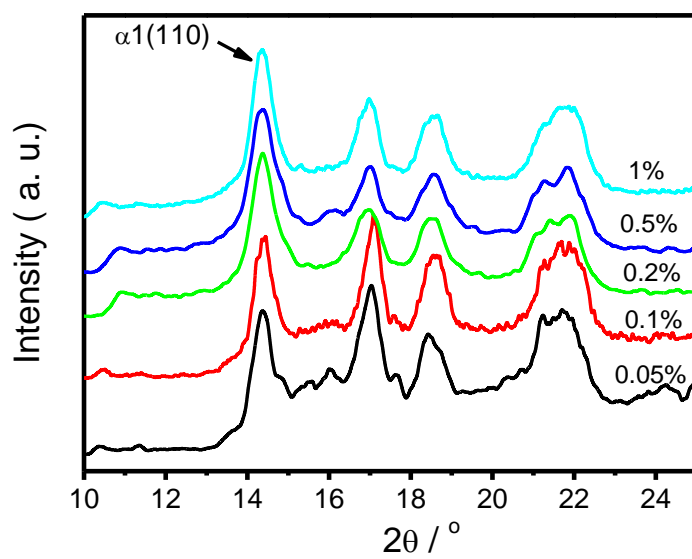


Figure 7 WAXD patterns of nucleated iPP with different TMB-5 contents crystallized at 145 °C